Characterization of a novel pH-stable GH3 β-xylosidase from *Talaromyces amestolkiae*: An enzyme displaying regioselective transxylosylation.

Manuel Nieto-Domínguez, Laura I. de Eugenio, Jorge Barriuso, Alicia Prieto, Beatriz Fernández de Toro, Ángeles Canales-Mayordomo, María Jesús Martínez*

Department of Environmental Biology, Centro de Investigaciones Biológicas, CSIC, Ramiro de Maeztu 9, E-28040 Madrid, Spain

*Corresponding author: María Jesús Martínez, Centro de Investigaciones Biológicas, Department of Environmental Biology, CSIC, Ramiro de Maeztu 9, E-28040 Madrid, Spain. Tel.: +34 918373112; fax: +34 915360432

E-mail address: mjmartinez@cib.csic.es

Running title: A new fungal β-xylosidase of biotechnological interest

Key words. Lignocellulosic biomass, xylan, enzyme, ascomycete

ABSTRACT

This paper reports on a novel β-xylosidase from the hemicellulolytic fungus *Talaromyces amestolkiae*. The expression of this enzyme, called BxTW1 could be induced by beechwood xylan and was purified as a glycoprotein from culture supernatants. We characterized the gene encoding this enzyme as an intron-less gene belonging to the Glycoside Hydrolase Gene Family 3 (GH 3). BxTW1 exhibited transxylosylation activity in a regioselective way. This feature would allow synthesizing oligosaccharides or other compounds not available from natural sources, such as alkyl glycosides displaying antimicrobial or surfactant properties. Regioselective transxylosylation, an uncommon combination, makes the synthesis reproducible, which is desirable for its potential industrial application. BxTW1 showed high pH stability and Cu^{2+} tolerance. The enzyme displayed a pI of 7.6, a molecular mass around 200 kDa in its active dimeric form and K_m and V_{max} values of 0.17 mM and 52.0 U/mg, respectively, using commercial *p*-nitrophenyl-β-D-xylopyranoside as substrate. The catalytic efficiencies for xylooligosaccharides hydrolysis were remarkably high, making it suitable for different applications in food and bioenergy industries.

INTRODUCTION

Plant biomass represents the most abundant renewable energy resource available on earth. It is mainly composed of cellulose and hemicellulose, two polysaccharides that constitute the raw material for the so-called second generation (2G) bioethanol industry. The production of this biofuel has received special attention in the last years because it is based on the use of non-food sources of cellulosic biomass (1). It has been pointed out that energy crops should be restricted to metal-contaminated soils in order to avoid edible cultivation competition against food industry (2, 3).

In order to make it economically viable, many modifications have been introduced in the industrial process during the last years. Among them, the strategy of combining enzymatic hydrolysis of lignocellulose with ethanol fermentation in a single process known as "Simultaneous Saccharification and Fermentation" (SSF) is a significant step forward, but it is still mandatory to reduce production costs and improve yields (1). Most studies have been using agricultural wastes as raw materials, usually after a physico-chemical pretreatment to disrupt lignocellulose structure to enhance cellulose and hemicellulose accessibility. Nevertheless, the industrial procedure currently set out to produce 2G ethanol consists in fermenting glucose, enzymatically released from cellulose using *Saccharomyces cerevisiae* as biocatalyst (4). To increase process yields, hemicellulose hydrolysis and pentoses fermentation are extremely relevant. Within this heterogeneous group of polysaccharides, xylans are the most abundant in hardwoods and grass. They are composed of a backbone of β-1,4-linked D-xylopyranosyl units highly substituted with arabinofuranose, glucose, glucuronic or methyl-glucuronic acid and acetyl side-groups. The enzymatic conversion of xylans into xylose at the industrial level is crucial to improve biomass conversion yield, although this aspect needs to be further developed (5). Due to their complexity and heterogeneity,

66 their complete breakdown requires the coordinated actions of several hydrolases, among
67 which endo-β-1,4-xylanases (EC 3.2.1.8) and β-xylosidases (EC 3.2.1.37) play
68 important roles. The first enzymes cut the xylan backbone into soluble oligosaccharides
69 that can be depolymerized to xylose by the action of β-xylosidases. There is a big
70 interest in identifying novel β-xylosidases since robust enzymes are needed for
71 lignocellulose biomass applications. In fact, most of the commercial enzymatic
72 preparations are deficient in this glycosyl hydrolase activity (6).

73 Hemicellulases can also be applied in many other industrial areas. For example,
74 a complete biodegradation of xylans is one of the goals for the paper industry since it
75 would improve the biobleaching process, hence reducing chlorine use. In the animal
76 feed area, β-xylosidase and other lignocellulolytic enzymes can be added to animal feed
77 in order to speed animals' weight gain. Endoxylanases and β-xylosidases hydrolyze
78 cereals' hemicelluloses facilitating nutrients mobility and promoting their absorption
79 (7).

80 β-xylosidases catalyze the hydrolysis of the glycosidic linkage by two possible
81 mechanisms. In the single displacement mechanism, a water molecule directly breaks
82 the bond, while the double displacement mechanism implies the formation of an
83 enzyme-substrate intermediate. In the first case, the released xylose suffers inversion of
84 its anomeric configuration, while the β configuration is kept if the second mechanism
85 occurs (8). According to the Carbohydrate Active enZymes database (CAZy,
86 http://www.cazy.org/), fungal β-xylosidases are belonging to three families: GH3,
87 GH43 and GH54. Family GH43 groups hydrolases with the inverting mechanism, while
88 families GH3 and GH54 include β-xylosidases with a retaining mechanism. Many
89 retaining β-xylosidases are capable of catalyzing the formation of a new glycosidic
90 linkage, transferring a xylosyl residue from a donor to an alcohol group of a particular

acceptor in a process called transxylosylation. This type of activity is especially interesting because this mechanism allows the synthesis of conventional as well as new xylooligosaccharides (XOs) of different degrees of polymerization (DP) with a potential outlet in prebiotics and interest for pharmacological applications (9). As an example, novel glycosidic-polyphenolic antioxidants with greater solubility and bioavailability can be be synthesized in such reactions (10).

Many cellulolytic and hemicellulolytic fungi belonging to the Ascomycota phylum have been described. Although *Aspergillus* and *Trichoderma* have been the most extensively studied, *Penicillium* strains seem to be good candidates as sources of lignocellulolytic enzymes (11). In a previous study, a perfect state (determined when fungal sexual phase is observed) of a *Penicillium* species, identified as *Talaromyces amestolkiae*, was selected for secreting a large amount of cellulases and hemicellulases (12).

This work reports the production, isolation and biochemical characterization of a β-xylosidase from *T. amestolkiae*. In addition, the sequencing and molecular characterization of the new enzyme are presented and its potential interest in hydrolysis and regioselective transxylosylation reactions is discussed.

MATERIALS AND METHODS

Fungal strain and culture media. The *T. amestolkiae* strain was isolated from cereal waste and deposited at the IJFM culture collection of the "Centro de Investigaciones Biológicas" (Madrid, Spain), with the reference A795.

Sporulation took place after culturing the fungus on 2% agar-malt Petri dishes at 26-28 ^{o}C for 7 days. About 1 cm^2 of agar-malt with growing mycelium was cut and added to a 5 mL solution of 1% NaCl and 0.1% Tween 80. The mixture was shaken and

200 µL were used to inoculate 250 mL flasks with 50 mL of CSS medium, containing (L^{-1}): 40 g glucose, 0.4 g $FeSO_4$ x $7H_2O$, 9 g $(NH_4)_2SO_4$, 4 g K_2HPO_4, 26.3 g corn steep solid, 7 g $CaCO_3$ and 2.8 mL soybean oil. pH was adjusted to 5.6 and the culture was incubated at 28 ºC and 180 rpm for 5 days.

β-xylosidase production was carried out in 250 mL flasks with 50 mL of Mandels medium and 2 mL of the CSS culture prepared for inoculum. Mandels medium contained (L^{-1}): 2.0 g KH_2PO_4, 1.3 g $(NH_4)_2SO_4$, 0.3 g urea, 0.3 g $MgSO_4 \cdot 7H_2O$, 0.3 g $CaCl_2$, 5 mg $FeSO_4 \cdot 7H_2O$, 1.6 mg $MnSO_4 \cdot H_2O$, 1.4 mg $ZnSO_4 \cdot 7H_2O$, and 1 g Bacto Peptone. Mandels medium was supplemented with 2% beechwood xylan (≥90% xylose), provided by Sigma-Aldrich, as carbon source and β-xylosidase inducer. Beechwood xylan is a hardwood xylan with a backbone of β-1,4-linked D-xylopyranosyl residues. Branches are mainly composed of 4-*O*-methylglucuronic acid attached to xylose C2 position and acetyl groups at C2 or C3 positions (13). In some experiments 1% or 3% xylan, 1% D-xylose 1% D-glucose or 1% Avicel (Merck) were used as alternative carbon sources. Cultures were incubated at 28 ºC and 180 rpm, and samples were periodically withdrawn from three replicate flasks and centrifuged at 20,000 × *g* for 5 min to separate the culture liquids from the mycelium.

Enzyme and protein assays. β-xylosidase activity was measured spectrophotometrically by the release of 4-nitrophenol (*p*NP) (ε_{410} = 15,200 M^{-1} cm^{-1}) from *p*-nitrophenyl-β-D-xylopyranoside (*p*NPX) (Sigma-Aldrich). The standard reaction mixture consisted of 3.5 mM *p*NPX, 50 mM sodium citrate buffer (pH 5), 0.1% bovine serum albumin (BSA), and the appropriate dilution of the purified enzyme or culture crude extract. Standard assays were incubated at 50 ºC and 500 rpm for 5 and 10 min, in order to check the linearity of the measured activity, and the reactions were

stopped by the addition of 500 µL 2% Na_2CO_3. Bovine serum albumin was added for stability issues. One unit of β-xylosidase activity was defined as the amount of enzyme that hydrolyzes 1 µmol of *p*NPX per minute.

Direct quantification of released xylose was performed either by gas chromatography-mass spectrometry (GC-MS) or spectrophotometrically, the latter using standards and reagents of the D-Xylose Assay Kit (Megazyme) and following the manufacturer indications.

For GC-MS analysis, xylose was previously converted into its alditol acetate derivative according to Notararigo *et al.* (14). Sample components were separately injected for identification on the basis of their retention time. Depending on the reactions, inositol or galactosamine were used as internal standard, to avoid overlapping with the reaction products.

The D-Xylose Assay Kit method is based on the complete conversion of free xylose into its beta anomer and then into D-xylonic acid, releasing NADH. Xylose concentration is determined by following NADH absorbance at 340 nm.

Hydrolytic activity against glucose-containing substrates was measured by quantifying free glucose after the enzymatic reactions. The measure was carried out colorimetrically through the coupling of glucose oxidase and peroxidase reactions using the Glucose-TR kit (Spinreact).

Proteins were quantified by the BCA method, using Pierce reagents and bovine serum albumin as standard, according to the manufacturer's instructions.

β-xylosidase purification. β-xylosidase production was carried out by culturing *T. amestolkiae* in 250 mL flasks with 50 mL of Mandels medium and 2% beechwood xylan as described above. 3-day-old cultures were harvested by filtering through filter

paper in order to separate mycelium from culture liquids. The filtrate was centrifuged at 10,000 × *g* and 4 ºC for 30 min and the supernatant filtered through 0.8, 0.45 and 0.22 μm disc filters (Merck-Millipore). Finally, the crude was concentrated and dialyzed against 10 mM acetate buffer (pH 4) using a 5-kDa cutoff membrane.

β-xylosidase was purified after three chromatographic steps using an ÄKTA Purifier chromatography system (GE Healthcare).

The dialyzed crude enzyme was loaded onto a 5 mL HiTrap SPFF cartridge (GE Healthcare), equilibrated in 10 mM sodium acetate buffer (pH 4). The bound proteins were eluted with a linear gradient of 1 M NaCl from 0 to 50% in 25 mL at a flow rate of 1 mL/min. The column was then washed with 1 M NaCl (10 mL), and allowed to re-equilibrate with the starting buffer for 10 min. Fractions with β-xylosidase activity were collected, desalted using PD-10 columns (GE Healthcare) equilibrated with 10 mM sodium acetate buffer (pH 4), and applied to a 1 mL Mono S 5/50 GL column (GE Healthcare) previously equilibrated in the same buffer. Proteins were eluted with a linear gradient of 1 M NaCl from 0 to 40% in 25 mL at a flow rate of 1 mL/min. The column was washed with 1 M NaCl (5 mL) and re-equilibrated to the starting conditions for 5 min. Fractions with β-xylosidase activity were collected, mixed, dialyzed and concentrated by ultrafiltration using Amicon Ultra-15 centrifugal devices (5 kDa cutoff, Merck-Millipore). Finally, samples were applied onto a Superose 12 HR 10/30 (GE Healthcare) equilibrated and eluted with the same buffer with 100 mM NaCl at a flow rate of 0.5 mL/min for 50 min. The purified enzyme was concentrated by ultrafiltration (5 kDa cutoff, Merck-Millipore) and stored at 4 ºC. The isolated β-xylosidase was named BxTW1.

Physicochemical properties. The molecular mass of BxTW1 was estimated by SDS-PAGE 7.5% acrylamide gels using Precision Plus Protein™ Dual Color Standards (Bio-Rad) and proteins were stained with Coomassie Brilliant Blue R-250 (Sigma-Aldrich). The molecular mass of the purified protein was also calculated from size exclusion chromatography on a Superose 12 HR 10/30 column previously calibrated with a standard protein kit (GE Healthcare) containing chymotrypsinogen A (19.5 kDa), ovalbumin (48.2 kDa), BSA (73.5 kDa), aldolase (170 kDa) and ferritin (460 kDa). Calibrants and samples were analyzed as described above. The accurate molecular mass and homogeneity of the pure enzyme were established by MALDI-TOF using an Autoflex III (Bruker Daltonics).

The isoelectric point of the protein was determined by isoelectrofocusing, in 5% polyacrylamide gels using pH 3-10 ampholytes (GE Healthcare), with 1 M H_3PO_4 and 1 M NaOH as anode and cathode buffers, respectively. The pH gradient was measured directly on the gel using a contact electrode (Crison). β-xylosidase activity was detected after incubation of the gels with 40 μM *p*-methylumbelliferyl β-D-xylopyranoside (Sigma-Aldrich) according to Yan *et al*. (15), visualizing *p*-methylumbelliferone fluorescence under UV light using the Gel Doc™ XR+ system (Bio-Rad).

The coding DNA sequence of the enzyme was used to predict the theoretical pI and molecular mass of the protein. To do so, it was first converted into an amino acidic sequence using the ExPASY Bioinformatic Resource Portal, submitting this sequence to the SignalP 4.1 server for identifying and locating the signal peptide, which was excluded from the mass prediction. Then, the mature protein sequence was analyzed using the Compute pI/Mw tool of the ExPASY Bioinformatic Resource Portal. The information was also submitted to The Eukaryotic Linear Motif resource (http://elm.eu.org/) in order to search for predicted post-translational modification sites.

The following parameters were selected: Extracellular, as Cell Compartment; *T. amestolkiae* as Taxonomic Context; and 100 as Motif Probability Cutoff.

N-carbohydrate content of β-xylosidase was demonstrated by the difference of the protein molecular mass before and after treatment with Endoglycosidase H (Roche), both estimated by SDS-PAGE in 7.5% polyacrylamide gels.

To find out the values of optimal temperature and pH, the ranges of temperature and pH stability, and the T50 of the purified enzyme, the standard reaction mixtures contained 120 mU/mL of BxTW1 (4.0 μg protein/mL) and 0.1% BSA to ensure the validity of the results regardless of the enzyme concentration. The particular conditions for each experiment are described below.

The optimal temperature of BxTW1 was determined incubating in a temperatures range from 30 to 70 ºC, for 5 and 10 min. The optimal pH was determined using a pH range from 2.2 to 9 at 50 ºC for 10 min. In order to adjust pH values, the sodium citrate buffer of the standard mix reaction was substituted by the one appropriate for each segment of the range: glycinate (2.2-3), formate (3-4), acetate (4-5.5), phosphate (5.5-7).

The T50 value, defined as the temperature at which the enzyme loses 50% activity after 10 min of incubation, was determined heating the protein in a range of temperatures from 45 to 75 ºC, cooling at 4 ºC for 10 min and rewarming to room temperature for 5 min before measuring the residual activity by the standard assay. The temperature at which the enzyme retained the maximum residual activity was taken as 100%.

β-xylosidase thermostability was studied incubating the purified enzyme in 10 mM sodium acetate buffer (pH 4) for 72 h at temperatures varying from 30 to 70 ºC. Samples were collected at different times and residual activity was assayed in standard

conditions. pH stability was analyzed in the range from 2.2 to 9 incubating the samples at 4 ºC for 72 h. In both assays, 100% corresponds to the initial activity.

The effect of common chemical compounds on β-xylosidase activity was studied by adding them to the reaction mix. LiCl, KCl, $AgNO_3$, $MgSO_4$, $CaCl_2$, $BaCl_2$, $MnCl_2$, $FeSO_4$, $CoCl_2$, $NiSO_4$, $CuSO_4$, $ZnSO_4$, $HgCl_2$, $Pb(NO_3)_2$, $AlNH_4(SO_4)_2$, $FeCl_3$ and ethylenediaminetetraacetic acid (EDTA) were assayed at a final concentration of 5 mM, while 2-mercaptoethanol (2-ME) and dithiothreitol (DTT) were added at a final concentration of 10 mM. The assay was carried out in standard conditions and in sodium acetate 50 mM (pH 5), to test the effect of the mild chelating effect described for sodium citrate (16).

Substrate specificity. The activity of pure BxTW1 was tested against the nitrophenyl substrates *p*NPX, *p*-NP-α-L-arabinopyranoside, *p*-NP-α-L-arabinofuranoside, *p*-NP-β-D-glucopyranoside, *o*-NP-β-D-glucopyranoside, *p*-NP-α-D-glucopyranoside, *p*-NP-α-L-rhamnopyranoside, *p*-NP-β-D-galactopyranoside, and *p*-NP-β-D-fucopyranoside (Sigma-Aldrich), at a final concentration of 3.5 mM. The activity of the enzyme was also assayed using as substrates 20 mM of the xylooligosaccharides xylobiose (X2), xylotriose (X3), xylotetraose (X4), xylopentaose (X5) and xylohexaose (X6) (Megazyme), and the disaccharides lactose, maltose, sucrose, lactose, gentiobiose and cellobiose (Sigma-Aldrich). Finally, the catalytic activity of BxTW1 against polysaccharides was evaluated using 20 mg/mL of beechwood xylan and laminarin from *Laminaria digitata* (Sigma-Aldrich). The assays were carried out at standard conditions and activity was measured by quantification of the released nitrophenol in the case of nitrophenyl substrates, xylose for xylooligosaccharides and beechwood xylan, and glucose for disaccharides and

laminarin. The concentration of released xylose and glucose were measured by using the D-Xylose Assay Kit and Glucose-TR kit, respectively, as described above.

The kinetic parameters of BxTW1 for each specific substrate were determined by using increasing substrate concentrations in a range from 0.078 to 20 mM. The experimental data derived from hydrolysis of *p*NPX, *p*NPAra, xylobiose, xylotriose, xylotetraose, xylopentaose, xylohexaose and beechwood xylan were adjusted by least squares to the Lineweaver-Burk linear equation of the Michaelis-Menten model. One unit of activity against XOS was defined as the amount of enzyme that totally hydrolyzes 1 μmol of the selected XOS to xylose per minute. Product inhibition by xylose was also studied and K_i determined against *p*NPX in the presence of 2.5, 5 and 10 mM xylose.

A deeper study of BxTW1 behavior using xylotriose as substrate was carried out by RMN spectroscopy. The assay consisted on incubating 20 mM xylotriose with 800 mU/mL of BxTW1 expressed in standard conditions, in 50 mM formate buffer (pH 3) at 25 ºC. The concentration of residual substrate and reaction products (disaccharide and monosaccharide) was followed by acquiring ^{1}H-NMR spectra at different reaction times, until detecting the complete conversion of xylotriose and xylobiose in xylose. The amounts of each compound were compared integrating distinctive signals: xylose was analyzed from H5 (δ 3.8), and xylotriose from H'5 (δ 4.03). Xylobiose lacked a specific signal in the ^{1}H-NMR spectrum, so it was quantified by subtracting xylotriose H'5 (δ 4.03) from H5 (δ 3.9), which overlaps the signals from xylobiose and xylotriose.

Transxylosylation reactions. The relationship between initial rates of transxylosylation and acceptor concentration was studied. Xylobiose and xylotriose in a range of concentrations from 1.25 to 80 mM were incubated with 200 mU/mL of

BxTW1 expressed in standard conditions and 50 mM formate buffer (pH 3) at 50 ºC for 10 min. The reaction was stopped by incubation at 100 ºC for 5 min. The presence and concentration of the remaining substrate, transxylosylation and hydrolysis products were determined by HPLC on an Agilent 1200 series system equipped with a refractive index detector.

Aliquots of 100 µL were loaded onto a SUPELCOGEL™ C-G610H column (Sigma) equilibrated in 5 mM H_2SO_4 buffer. The column was previously calibrated injecting 100 µL of xylose and XOs samples, from X2 to X5, in a concentration range from 0.5 mM to 20 mM. From the area under the peaks, a calibration curve was calculated for each compound. Peaks were identified from their retention times, by comparison with those of the commercial standards, and their concentration calculated from the calibration curves. The results were used to estimate hydrolysis and transxylosylation ratios according to the equations below:

$$\frac{([Substrate]_0 - [Substrate]_f) - 2[Transxylosylation\ product]_f}{[Substrate]_0 - [Substrate]_f} X100$$

$$= Hydrolysis\ ratio$$

$$100 - Hydrolysis\ ratio = Transxylosylation\ ratio$$

In order to evaluate the acceptor specificity of the enzyme, 3.5 mM *p*NPX (as xylose donor) was incubated for 240 min with 24 mU/mL of BxTW1, expressed in standard conditions, and 50 mM formate buffer (pH 3), in the presence of one of the following acceptors: 1 M methanol, ethanol, 1-propanol, 2-propanol, 1-butanol, isobutanol or glycerol, or 70 mg/mL erythritol, mannitol, sorbitol, dulcitol, glucose, fructose, galactose, mannose, maltose, sucrose, trehalose or lactose. The selected acceptors were compared and grouped according to their physicochemical similarity after calculating the Tanimoto coefficient, using the workbench similarity tool from the

ChemMine site (17). The reaction was stopped by incubation at 100 ºC for 5 min. The amount of free *p*NP released from substrate hydrolysis was measured spectrophotometrically, while xylose content was determined by GC-MS, as described above. Transxylosylation, substrate hydrolysis and substrate consumption ratios were calculated from the concentration of xylose and *p*NP according to the equations below:

$$\frac{[p\mathrm{NPX}]_0 - [p\mathrm{NP}]_{\mathrm{free}}}{[p\mathrm{NPX}]_0} \times 100 = \text{Substrate consumption}$$

$$\frac{[p\mathrm{NP}]_{\mathrm{free}} - [\mathrm{xylose}]_{\mathrm{free}}}{[p\mathrm{NP}]_{\mathrm{free}}} \times 100 = \text{Transxylosylation ratio}$$

$$100 - \text{Transxylosylation ratio} = \text{Hydrolysis ratio}$$

The results were presented as a heat map based on transxylosylation ratios. The hierarchical clustering analysis was performed using the clustergram algorithm within Matlab environment (MathWorks, Natick, MA).

BxTW1 regioselectivity when catalyzing the formation of a new glycosidic linkage was also investigated. In order to obtain one or more transxylosylation products, 350 mM xylobiose was incubated in 50 mM formate buffer (pH3) at 50 ºC for 30 min with 550 mU/mL of BxTW1. In a second experiment, 3.5 mM of *p*NPX was used as donor and 130 mM of xylose as acceptor, incubating with 500 mU/mL of BxTW1 in 50 mM formate buffer (pH 3), at 50 ºC for 20 min, in order to obtain one or more transxylosylation products. Both reactions were stopped by heating at 100 ºC for 5 min. Samples were dried and resuspended in deuterated water. The identification of the transxylosylation products was accomplished by ^{1}H, ^{1}H-^{13}C HSQC, DOSY and DOSY-TOCSY-NMR on a Bruker 600 MHz spectrometer. The same approaches were applied to the commercial reagents added to each reaction, in order to discard signals from impurities and to confirm the assignations.

Peptide mass fingerprinting using MALDI-TOF mass spectrometry. Gel pieces of the BxTW1 protein bands from Sypro-stained SDS-gels were excised and digested following a protocol based on Shevchenko *et al.* (18) with the minor variations reported by Russo *et al.* (19). MALDI–MS and MS/MS data were combined through the BioTools 3.0 program (Bruker-Daltonics) to interrogate the NCBI non-redundant protein database (NCBI: 20100306) using MASCOT software 2.3 (Matrix Science). Relevant search parameters were set: trypsin as enzyme, carbamidomethylation of cysteines as fixed modification, methionine oxidation as variable modification, 1 missed cleavage allowed, peptide tolerance of 50 ppm and MS/MS tolerance of 0.5 Da. Protein scores greater than 75 were considered significant ($P<0.05$).

Primer design, amplification of BxTW1 and classification. To identify the gene coding for BxTW1, a Blastp search against NCBInr using the peptides obtained by mass fingerprinting was carried out. The nucleotide sequences of the genes coding for β-xylosidases with high sequence identity to BxTW1 were retrieved from the database. Sequences were aligned using ClustalW and degenerate primers were designed in the conserved 5' and 3' regions, including ATG and Stop codons (BxTw1 Fw 5'-ATGGTYTACACCRYGCAATWYCTG -3' and BxTw1 Rv 5'-TYAMYTRKRATCAGGYTKAATCTCC -3'). The *bxtw1* gene was amplified by polymerase chain reaction (PCR) using genomic DNA as template. The DNA was extracted with DNeasy Plant Mini Kit (QIAGEN), and PCR reactions contained 100 ng of DNA template, 1X PCR Buffer, 1.5 mM $MgCl_2$, 0.8 mM dNTPs, 0.5 μM of each primer and 1 U of Taq DNA polymerase (Invitrogen) in a final volume of 50 μL. Reactions were subjected to an initial denaturation at 94 °C for 5 min, 34 cycles of

amplification, each at 94 °C for 45 s, then 55 °C for 45 s and 72 °C for 2.5 min, followed by a final extension step at 72 °C for 5 min. Control reactions lacking template DNA were simultaneously performed.

The amplified sequences were separated in a 0.8% w/v agarose electrophoresis gel stained with GelRed, cut out, and purified by QIAquick Gel Extration Kit (QIAGEN). PCR products were then inserted into pGEM-T easy cloning system (Promega) in order to transform the *Escherichia coli* DH5α strain. Clones containing the inserted fragments were sequenced using the BigDye Terminator v3.1 Cycle Sequencing kit, and the automated ABI Prism 3730 DNA sequencer.

The translated coding sequence was used to carry out a Blastn search against the NCBInr, in order to identify homologous proteins and include BxTW1 in the appropriate GH family.

RESULTS

β-xylosidase production. The secreted proteins and β-xylosidase activity of *T. amestolkiae* cultures were studied in Mandels medium with different carbon sources. Figure 1A shows the β-xylosidase-inducer effect of 1% Avicel, 1% D-xylose or 1%, 2% or 3% beechwood xylan during 6 days. A control culture with 1% D-glucose as carbon source, which inhibits xylanases production by carbon catabolite repression (20), was also tested. The highest β-xylosidase activity was detected when 2% beechwood xylan was used as inductor, and the profile of total secreted proteins was similar to those detected with 3% xylan. Xylose addition also produced β-xylosidase release, although at a lower level. Figure 1B depicts the levels of secreted proteins during the culture time, showing a sharp increase of extracellular proteins at the end of the period. At this point, a very fragmented mycelium was observed under the light microscope (data not

shown), probably related to cellular lysis and massive release of intracellular proteins. Based on these results, 2% beechwood xylan was chosen as the best inducer for β-xylosidase, which was produced, purified and characterized from these crudes. For additional data on the high abundance of BxTW1 in the secretome of *T. amestolkiae*, under the conditions selected here, see Fig. S1 and "Secretome" section in Supplemental Material.

Purification of β-xylosidase. Maximal β-xylosidase activity levels (800 mU/mL) were detected in 3-day-old cultures. Then, these crudes were collected for enzyme purification.

The first cation exchange chromatography step allowed the separation of a unique peak with β-xylosidase activity, eluting around 0.25 M NaCl, from most of the crude proteins. The peak with β-xylosidase activity was subsequently separated on Mono S 5/50, a high-resolution cation exchange column. β-xylosidase activity mainly eluted in three successive peaks between 0.20 and 0.25 M NaCl. A last step using a high-resolution Superose 12 column was necessary for the complete purification of the protein, denominated BxTW1. The enzyme, dialyzed and concentrated, was stored at 4 ºC, remaining stable during at least six months.

The purification resulted in a final yield of 10.8% recovered activity. During the process, the specific activity increased from 1.0 to 47.1 U/mg, which implies a degree of purification of 46.6.

Physicochemical properties. The molecular mass (M_w) of BxTW1, estimated from size exclusion chromatography, was around 200 kDa. However, analysis of the BxTW1 sequence (GenBank ID: KP119719) using the ExPASY Bioinformatics

Resource Portal resulted in a theoretical molecular mass of 84,373.96 Da. SDS-PAGE of non-deglycosylated BxTW1 showed three bands of approximately 100 kDa (Fig. 2A), which is close to the value from MALDI-TOF-MS (Fig. 2B). The MALDI-TOF spectrum displayed the typical profile of a glycosylated protein, with a wide peak due to glycosylation heterogeneity. The technique allowed determining the accurate mass of one of the glycosylated isoforms (102,275 kDa) but the global enzyme mass could only be estimated on average around 100 kDa. The closeness of the peaks in the mass spectrum apparently corresponded to three different glycosylation forms, which would be consistent with the identification of three separated peaks of β-xylosidase activity during high-resolution cation exchange chromatography. The peptide mass fingerprint of each one of the three bands was obtained, resulting in exactly the same fragmentation patterns (not shown). To discern if these molecular weight changes could be due to glycosidic content variations, the mature protein sequence was used to search for predicted post-translation modifications at ELM server, and 14 motifs for N-glycosylation were found. In addition, after EndoH treatment only one peak was detected, with a molecular mass close to the theoretical value of 84 kDa, corroborating the existence of three different glycosylation isoforms of BxTW1 instead of three different isoenzymes. The difference between the molecular mass determined by size exclusion chromatography and SDS-PAGE suggests that BxTW1 works as a non-covalent dimer in its native conformation.

Isoelectrofocusing indicated that pI of the protein was 7.6, a similar value to those reported for other β-xylosidases (20). Nevertheless, the theoretical value obtained from BxTW1 sequence was 4.75. This difference was not surprising since there has been extensively reported that glycosylation can change the isoelectric point of a protein (21).

The influence of temperature and pH on stability and optimal reaction activity of BxTW1 was tested against *p*NPX. The optimum temperature (highest hydrolysis rate) was 70 ºC, although the enzyme lost 70% activity after 30 min at 60 ºC (data not shown). At 50 ºC, the activity loss stabilized around 50% after 1 h (data not shown) and remained stable for 72 h (Fig. 3A). The thermal index T50 was 59.9 ºC.

Regarding pH, BxTW1 displayed its maximal activity at pH 3 and exhibited high stability (above 80% of residual activity) between pH 2.2 and 9 for 72 h (Fig. 3B).

BxTW1 activity did not show relevant changes in the presence of most of the tested compounds using sodium acetate or citrate buffers at pH 5 (Fig. 4). When small inhibition rates were observed, the residual activities were slightly higher in the presence of citrate, probably due to its chelating properties. The most remarkable results were the slight inhibition registered during the addition of Cu^{2+} and Pb^{2+} in both buffers and the dramatic decrease of activity in the presence of Hg^{2+}. The absence of inhibition in the presence of EDTA, dithiothreitol and 2-mercaptoetanol suggest that BxTW1 does not require metallic cations for its catalytic activity and the absence of a disulfide bond near or inside the active site. The non-dependence of metal cofactors is a common feature of GH3 proteins, but there are a few solved structures displaying disulfide bonds within this group (22, 23).

Substrate specificity. The enzyme hydrolyzed *p*NPX, *p*NP-α-L-arabinopyranoside, *p*NP-α-L-arabinofuranoside, xylooligosaccharides (XOs) from X2 to X6, and was capable of releasing xylose from beechwood xylan. Nevertheless, no activity was detected on other nitrophenyl substrates or disaccharides assayed. The kinetic parameters of BxTW1 (Table 1) were determined using the specific substrates reported above. Although the enzyme was able to hydrolyze *p*NP-α-L-arabinoside

457 independently of the glycon moiety configuration, its affinity towards these substrates
458 was much lower than that found for *p*NPX. The hydrolytic mechanism of BxTW1 was
459 ascertained by ^{1}H-NMR, analyzing xylose release during the first minutes of reaction.
460 As all the GH3 family members, BxTW1 worked with a retaining mechanism (for the
461 RMN data see the "Analysis of the hydrolytic mechanism of BxTW1" section in
462 Supplemental Material). The enzyme also hydrolyzed XOs of different chain length,
463 with similar affinity from 3 to 6 xylose units, but with decreasing catalytic efficiency.
464 Surprisingly, the enzyme attacked X3-X6 with higher affinity than X2. Since K_m values
465 were calculated by estimating released xylose instead of monitoring substrate
466 consumption, and in order to confirm that BxTW1 hydrolyzed X3 preferentially over
467 X2, xylotriose consumption and xylobiose generation were followed ^{1}H-NMR
468 spectroscopy (Fig. 5A). Comparison of spectra revealed the preference of BxTW1 for
469 the trisaccharide over the released disaccharide (Fig. 5B). This result unequivocally
470 demonstrated xylotriose consumption and agreed with global K_m values for XOs
471 calculated from the xylose released. Enzyme inhibition by product was also studied,
472 revealing that the activity against *p*NPX was competitively inhibited by xylose, with a
473 K_i of 1.7 mM.
474
475 **Transxylosylation.** The transxylosylation capabilities of BxTW1 were tested.
476 Xylotriose or xylobiose were firstly assayed as simultaneous donors and acceptors in
477 separated reactions. This double role of substrates has been previously reported (24).
478 Since the enzyme preferentially hydrolyzes X3 over X2 (Fig. 5), differences in
479 transxylosilation rates were also analyzed as a function of the acceptor length and
480 concentration. In this work, a direct relation between acceptor concentration and the
481 synthesis of transxylosylation products was observed (Fig. 6). On the other hand,

xylotriose was synthetized from xylobiose and, when xylotriose was used as the substrate, the resultant product was xylotetraose. In both cases transxylosylation ratios increased with the substrate concentrations (detection limit above 5 mM substrate). Below 10 mM, transxylosylation rates were comparable using X2 or X3. However, X2 was better transxylosylation acceptor than X3 at concentrations over 20 mM (about 40% transxylosylation rate versus 30%, respectively). Figure 6 shows the evolution of transxylosylation and hydrolysis ratios using xylobiose (Fig. 6A) and xylotriose (Fig. 6B) as substrates.

The transxylosylation specificity of BxTW1 was tested in reactions with *p*NPX as donor and a large excess of different acceptors, measuring xylose/*p*NP ratios at the final reaction time. To calculate transxylosylation rates, the stoichiometric relation between products (xylose and *p*NP) was taken as 1:1. Then, detection of *p*NP in a significantly higher concentration than xylose for an assayed acceptor indicates that transxylosylation occurred and the monosaccharide has been attached to the acceptor. A variety of alkyl alcohols, sugar alcohols, monosaccharides and disaccharides were tested as acceptors. A small transxylosylation rate of 13% was observed in the absence of acceptor, showing that BxTW1 was capable of using *p*NPX molecules as acceptors. The consumed substrate exceeded 80% in all cases, and the highest transxylosylation rates were obtained mainly with alkan-1-ols, alkan-2-ols, and sugar alcohols (Fig. 7A), while monosaccharides and disaccharides turned out to be the worst acceptors. Chemical similarities between acceptors were estimated by Tanimoto coefficient calculation and a comparative analysis was carried out using the hierarchical clustering tool from the MatLab environment (Fig. 7B). The results showed that compounds with very close physicochemical features behave differently as transxylosylation acceptors. Regarding sugar alcohols, mannitol is a much better acceptor than sorbitol and dulcitol although all

of them have the same molecular formula. In the case of aldoses, glucose, galactose and mannose also share the same empirical formula, but were very different as acceptors: glucose was the most efficient, while transxylosylation yields for galactose were significant lower.

Regioselectivity of BxTW1 when catalyzing the formation of a new glycosidic linkage, using xylobiose or xylose as acceptor, was also investigated. Xylobiose was used as simultaneous donor and acceptor for the synthesis of either the trisaccharide or higher DP transxylosylation products. A DOSY-NMR spectrum of the reaction mixture was acquired, and the detected signals could be correlated with the presence of mono-, di- and trisaccharides. DOSY-TOCSY and ^{1}H-^{13}C HSQC-NMR spectra were acquired in order to simplify the assignation of ^{1}H 1D-NMR signals. The chemical-shift displacement data allowed concluding that BxTW1 catalyzed the regioselective synthesis of 1,4-β-D-xylotriose as unique transxylosylation product. BxTW1 regioselectivity was also tested using *p*NPX as donor and xylose as acceptor, to test if the reaction products were disaccharides or had higher DPs. A ^{1}H-NMR spectrum was acquired from the reaction mix and ^{1}H-^{13}C HSQC-NMR data were used to simplify the analysis. The assignation of signals indicated that BxTW1 catalyzed the synthesis of 1,4-β-D-xylobiose, as the unique transxylosylation product.

Sequencing, classification and molecular characterization of BxTW1. The preliminary identification of BxTW1 was based on its peptide mass fingerprint. The three bands identified in SDS-PAGE gels as glycosylated isoforms of BxTW1were analyzed, giving the same profile of tryptic peptides. The homology search of these peptides revealed the closeness of BxTW1 with four putative fungal β-xylosidases from *Talaromyces stipitatus* ATCC 10500 (gi:242771939), *Talaromyces cellulolyticus*

(gi:348604625) *Talaromyces marneffei* ATCC 18224 (gi:212531051) and *Hypocrea orientalis* strain EU7-22 (gi:380293099), and three β-xylosidases isolated from *Trichoderma reesei* (gi:2791277), *Talaromyces emersonii* (gi:48526507) and *Aspergillus fumigatus* (gi:76160897), respectively.

Gene sequencing revealed that a 2394 bp region with no introns codifies for BxTW1. The nucleotide sequence was submitted to the GenBank database with accession number KP119719. An homology search based on DNA sequence showed its high identity with putative β-xylosidases from *T. stipitatus* ATCC 10500 (gi:242771939), *T. cellulolyticus* (gi:348604625) and *T. marneffei* ATCC 18224 (gi:212531051), all of them belonging to the GH3 family and lacking introns.

These data indicate that BxTW1 from *T. amestolkiae* is a β-xylosidase from the GH 3. For the phylogenetic validation of this classification see Fig. S2 and the "Identification of BxTW1 GH family" section in Supplemental Material.

DISCUSSION

The identification and characterization of β-xylosidases are currently outstanding topics. The needs for biomass exploitation in order to obtain goods from renewable sources and the synthesis of xylooligosaccharides by transxylosylation make these enzymes very interesting from a biotechnological perspective.

In this context, the β-xylosidase levels released by *T. amestolkiae* in liquid cultures are in agreement with previous results described for *Aspergillus* and *Fusarium* strains when beechwood xylan was added as carbon source (25, 26), and higher than those reported for other *Penicillium* species (27, 28). Although pure commercial xylan is not suitable for high-scale enzyme production, it has been established as the most used carbon source and the best inducer of xylanolytic enzymes (29). As in other fungi,

557 xylose acts as a weak inducer of β-xylosidase production in *T. amestolkiae* (30), but
558 glucose did not induce β-xylosidase production (30, 31).

559 The study of the effect of temperature, pH and common chemicals on BxTW1
560 activity revealed some remarkable properties. The optimum pH value of 3.0 was
561 surprising since most of the described fungal β-xylosidases displayed values from 4.0 to
562 6.0 (20) and few enzymes with this optimum value (32) or lower (33) have been
563 described. The causes for this value remain unknown. Sequence alignments of BxTW1
564 and closely related GH3 xylosidases (data not shown) revealed no changes in the
565 catalytic environment that would explain the low optimum pH of BxTW1. However,
566 Rasmussen *et al.* (34) reported that β-xylosidases from *T. emersonii* and *T. reesei*
567 changed their optimum pH from 4.0 to 3.0-3.5 when expressed in *Aspergillus oryzae*,
568 for which high N-glycosylation potential has been reported (35). This observation could
569 suggest that this post-translational modification might modulate pH-sensitivity of
570 glycosyl-hydrolases. N-oligosaccharides may display charged substituents (36) which
571 could affect pH-sensitivity by changing the pI or modifying pKa value of close
572 aminoacids. In the case of BxTW1, N-glycosylation has been by SDS-PAGE after
573 EndoH treatment and by *in silico* analysis, concluding that the reported difference
574 between theoretical and experimental pI could be explained by these modifications.
575 According to these findings, the low optimum pH of BxTW1 could also be related to its
576 glycosylation pattern, and not to changes in the aminoacidic sequence of the active site.
577 The broad stability pattern of the *T. amestolkiae* enzyme was also notable, covering
578 acidic and basic values, while most of the characterized fungal β-xylosidases are
579 quickly inactivated at extreme (low or high) pH values (26, 37). Both stability and high
580 activity at low pH values make it a good candidate to be used in 2G-bioethanol
581 production or as supplements for animal feed.

582 The absence of BxTW1 inhibition in the presence of several heavy metals
583 commonly inactivating β-xylosidases merits especial attention. The resistance is
584 particularly important in the case of Cu^{2+}, which has been reported as a strong inhibitor
585 of many β-xylosidases (38, 39) present in the ash content of different lignocellulosic
586 biomasses, showing inhibitory effects on cellulases and reducing the final yield of 2G
587 bioethanol production even at low concentrations (40).
588 Regarding its kinetic characterization, although the maximum velocity of
589 BxTW1 was comparable to those reported for other fungal β-xylosidases (Table 2), the
590 results showed a remarkable high affinity of the enzyme to *p*NPX. Very few
591 characterized β-xylosidases, as BXTE from *T. emersonii* (34), had a slightly lower K_m
592 value towards this substrate. Nevertheless, BxTW1 demonstrated better kinetic
593 properties: its V_{max} is 22-fold higher compared with Xyl I and the k_{cat} against *p*NPX was
594 173 s^{-1}, more than 700-fold higher than the reported for BXTE. Catalytic efficiency, an
595 extensively used parameter for enzyme comparison (41) is also shown for each enzyme,
596 when available, in Table 2. The efficiency of BxTW1 showed to be among the highest
597 values reported. In fact, β-xylosidase from *Bacillus pumilus*, commercialized by
598 Megazyme (SKU code E-BXSEBP), shows a catalytic efficiency of 230 $mM^{-1}\cdot s^{-1}$,
599 calculated from the reported data (42), a value 4.5-fold lower than that of BxTW1.
600 Although the activity of the enzyme towards xylobiose is in the range of the
601 highest values found in literature (43), it showed higher affinity towards longer
602 substrates (X3-X6). Even though kinetic characterization of β-xylosidases against XOS
603 with a DP higher than xylobiose has not been deeply studied, a detailed comparison
604 revealed that BxTW1 had the highest catalytic efficiency for all the XOs tested from X3
605 to X6. In fact, the kinetic constants of BxTW1were frequently one or two orders of
606 magnitude over those of characterized β-xylosidases (Table 3). In addition, BxTW1

607 showed activity against beechwood xylan, something uncommon among most of the
608 known β-xylosidases. These behaviors have been previously reported and they are
609 considered a typical feature of exo-type xylanolytic enzymes (34, 44), in opposition to
610 classical β-xylosidases (45). Exo-type xylanases (EC 3.2.1.156) are also called reducing
611 end xylose-releasing exo-oligoxylanases (Rex enzymes) and they share with β-
612 xylosidases (EC 3.2.1.37) the exo-attack of substrates. Nevertheless, there are several
613 differences suggesting that BxTW1 should be identified as a β-xylosidase. As
614 mentioned above, alignment studies displayed high homology between BxTW1 and
615 other putative and characterized β-xylosidases. In addition, all the reported Rex
616 enzymes are included in GH8 family, work with inversion of the configuration and are
617 unable to hydrolyze xylobiose (46). These data strongly suggest that BxTW1 cannot be
618 considered as a Rex enzyme, and should be considered a β-xylosidase.

619 BxTW1 demonstrated transxylosylation capacity, and rates increased with
620 substrate concentration when xylobiose and xylotriose were used as donor and acceptor
621 simultaneously. The transxylosylation and hydrolytic rates were complementary, since
622 the longest substrate was a worse acceptor than the shortest.

623 BxTW1 showed broad acceptor specificity. Short alkan-ols were the best
624 acceptors, probably due to their low molecular mass and to the physicochemical
625 properties of the enzyme's active site, as its size or hydrophobicity. The results
626 suggested that aldoses and alcohols were preferentially transxylosylated on primary
627 alcohols, since 1-propanol and 1-butanol were better acceptors than 2-propanol and
628 isobutanol, respectively. To confirm this, aldohexoses distinguished only by their three-
629 dimensional spatial orientation were used as acceptors. In D-glucose all hydroxyl
630 groups but the primary one (C6) are in equatorial position and, hence, the
631 transxylosylation rates were higher than those obtained with D-mannose, where C2

hydroxyl group shares the axial position with the primary alcohol. The transxylosylation rate was even lower when D-galactose was used as acceptor, where the axial position was occupied by C4 hydroxyl (closer than C2 to the primary alcohol). No clear conclusions could be drawn from the results obtained when sugar alcohols or disaccharides were used as acceptors; in these cases, unknown steric hindrances may occur. A deeper understanding of the residues and mechanism involved in transxylosylation reactions would be necessary to decipher acceptor specificity (24, 47). Currently, a complete structural analysis of BxTW1 is being carried out in order to grasp its hydrolytic and transxylosylation capacities.

Both, promiscuity and efficiency, suggest a considerable potential of BxTW1 for the biosynthesis of oligosaccharides with pharmacological or industrial interest. The enzymatic synthesis of new oligosaccharides by transglycosylation is a promising alternative to chemical methods. Many glycosidases have been studied in order to determine their ability to form a glycosidic bond stereospecifically, but most of them show a low regioselectivity. This implies that the transglycosylation products are multiple instead of uniques, hence hampering their use for industrial production. Few regioselective glycosidases have been described and it has been related with their specificity (48). In this sense, although BxTW1 regioselectivity has been analyzed only when xylose or xylobiose were used as acceptors, its broad substrate specificity make it a good candidate to test different and new molecules as final xylose receivers. This reinforces the potential of BxTW1 for the biosynthesis of new oligosaccharides with potential industrial interest.

ACKNOWLEDGEMENTS

This work has been carried out with funding from the MINECO projects PRI-PIBAR-2011-1402 and RTC-2014-1777-3 and the Comunidad de Madrid Program RETO-PROSOT S2013/MAE-2907. M. Nieto thanks the MINECO for a FPU fellowship. The authors thank F.J. Cañada and J. Jiménez-Barbero for their help in the development of NMR experiments and J. Nogales for his help in the development of hierarchical clustering analysis. The authors thank the Gas Chromatography and Proteomics and Genomic facilities at CIB.

REFERENCES

1. **Naik S, Goud VV, Rout PK, Dalai AK**. 2010. Production of first and second generation biofuels: A comprehensive review. Renew Sustain Energy Rev **14**:578-597.

2. **Zhang X, Zhu Y, Zhang Y, Liu Y, Liu S, Guo J, Li R, Wu S, Chen B**. 2014. Growth and metal uptake of energy sugarcane (*Saccharum spp*.) in different metal mine tailings with soil amendments. J Environ Sci (China) **26**:1080-1089.

3. **Xie J, Weng Q, Ye GY, Luo SS, Zhu R, Zhang AP, Chen XY, Lin CX**. 2014. Bioethanol Production from Sugarcane Grown in Heavy Metal-Contaminated Soils. Bioresources **9**:2509-2520.

4. **Talebnia F, Karakashev D, Angelidaki I**. 2010. Production of bioethanol from wheat straw: An overview on pretreatment, hydrolysis and fermentation. Bioresour Technol **101**:4744-4753.

5. **Kuhad RC, Gupta R, Khasa YP, Singh A, Zhang Y**. 2011. Bioethanol production from pentose sugars: Current status and future prospects. Renew Sustain Energy Rev **15**:4950-4962.

6. **Bao L, Huang Q, Chang L, Sun Q, Zhou J, Lu H**. 2012. Cloning and characterization of two beta-glucosidase/xylosidase enzymes from yak rumen metagenome. Appl Biochem Biotechnol **166**:72-86.

7. **Pastor, F., O. Gallardo, J. Sanz-Aparicio, and P. Drouet**. 2007. Xylanases: Molecular properties and applications, p. 65-82. *In* J. Polaina and AP. McCabe (eds.), Industrial Enzymes: Structure, Function and Applications. Springer.

8. **Rye CS, Withers SG**. 2000. Glycosidase mechanisms. Curr Opin Chem Biol **4**:573-580.

9. **Azevedo Carvalho AF, Oliva Neto P, Da Silva DF, Pastore GM**. 2013. Xylo-oligosaccharides from lignocellulosic materials: Chemical structure, health benefits and production by chemical and enzymatic hydrolysis. Food Res Int **51**:75-85.

10. **Torres P, Poveda A, Jimenez-Barbero J, Luis Parra J, Comelles F, Ballesteros AO, Plou FJ**. 2011. Enzymatic Synthesis of alpha-Glucosides of Resveratrol with Surfactant Activity. Advanced Synthesis & Catalysis **353**:1077-1086.

11. **Chavez R, Bull P, Eyzaguirre J**. 2006. The xylanolytic enzyme system from the genus *Penicillium*. J Biotechnol **123**:413-433.

12. **Gil-Muñoz J**. 2015. Estudio de las β-glucosidasas del complejo celulolítico de *Talaromyces amestolkiae*: Caracterización y aplicaciones biotecnológicas. Thesis, Universidad Complutense, Madrid.

13. **Freixo MR, de Pinho MN**. 2002. Enzymatic hydrolysis of beechwood xylan in a membrane reactor. Desalination **149**:237-242.

14. **Notararigo S, Nácher-Vázquez M, Ibarburu I, Werning ML, de Palencia PF, Dueñas MT, Aznar R, López P, Prieto A**. 2013. Comparative analysis of production and purification of homo- and hetero-polysaccharides produced by lactic acid bacteria. Carbohydr Polym **93**:57-64.

15. **Yan Q, Wang L, Jiang Z, Yang S, Zhu H, Li L**. 2008. A xylose-tolerant beta-xylosidase from *Paecilomyces thermophila*: Characterization and its co-action with the endogenous xylanase. Bioresour Technol **99**:5402-5410.

16. **Wasay SA, Barrington SF, Tokunaga S**. 1998. Remediation of soils polluted by heavy metals using salts of organic acids and chelating agents. Environ Technol **19**:369-379.

17. **Backman TW, Cao Y, Girke T**. 2011. ChemMine tools: an online service for analyzing and clustering small molecules. Nucleic Acids Res **39**:W486-W491.

18. **Shevchenko A, Tomas H, Havlis J, Olsen JV, Mann M**. 2006. In-gel digestion for mass spectrometric characterization of proteins and proteomes. Nat Protoc **1**:2856-2860.

19. **Russo P, de la Luz Mohedano M, Capozzi V, Fernandez de Palencia P, Lopez P, Spano G, Fiocco D**. 2012. Comparative Proteomic Analysis of Lactobacillus

721 plantarum WCFS1 and Delta ctsR Mutant Strains Under Physiological and Heat
722 Stress Conditions. International Journal of Molecular Sciences **13**:10680-10696.

723 20. **Knob A, Terrasan C, Carmona E**. 2010. beta-Xylosidases from filamentous
724 fungi: an overview. World J Microbiol Biotechnol **26**:389-407.

725 21. **Marsh JW, Denis J, Wriston JC**. 1977. Glycosylation of *Escherichia coli* L-
726 Asparaginase. Journal of Biological Chemistry **252**:7678-7684.

727 22. **Varghese JN, Hrmova M, Fincher GB**. 1999. Three-dimensional structure of a
728 barley beta-D-glucan exohydrolase, a family 3 glycosyl hydrolase. Structure
729 **7**:179-190.

730 23. **Suzuki K, Sumitani Ji, Nam YW, Nishimaki T, Tani S, Wakagi T, Kawaguchi**
731 **T, Fushinobu S**. 2013. Crystal structures of glycoside hydrolase family 3 beta-
732 glucosidase 1 from *Aspergillus aculeatus*. Biochem J **452**:211-221.

733 24. **Kurakake M, Fujii T, Yata M, Okazaki T, Komaki T**. 2005. Characteristics of
734 transxylosylation by beta-xylosidase from *Aspergillus awamori* K4. Biochim
735 Biophys Acta Gen Subj **1726**:272-279.

736 25. **Lenartovicz V, de Souza CGM, Moreira FG, Peralta RM**. 2003. Temperature
737 and carbon source affect the production and secretion of a thermostable β-
738 xylosidase by *Aspergillus fumigatus*. Process Biochem **38**:1775-1780.

739 26. **Saha BC**. 2001. Purification and characterization of an extracellular beta-
740 xylosidase from a newly isolated *Fusarium verticillioides*. J Ind Microbiol
741 Biotechnol **27**:241-245.

27. **Jørgensen H, Mørkeberg A, Krogh KBR, Olsson L**. 2005. Production of cellulases and hemicellulases by three *Penicillium* species: effect of substrate and evaluation of cellulase adsorption by capillary electrophoresis. Enzym Microb Technol **36**:42-48.

28. **Knob A, Carmona EC**. 2011. Purification and properties of an acid beta-xylosidase from *Penicillium sclerotiorum*. Ann Microbiol **62**:501-508.

29. **Milagres AMF, Lacis LS, Prade RA**. 1993. Characterization of xylanase production by a local isolate of *Penicillium janthinellum*. Enzym Microb Technol **15**:248-253.

30. **Jørgensen H, Mørkeberg A, Krogh KBR, Olsson L**. 2004. Growth and enzyme production by three *Penicillium* species on monosaccharides. J Biotechnol **109**:295-299.

31. **Terrasan CRF, Temer B, Duarte MCT, Carmona EC**. 2010. Production of xylanolytic enzymes by *Penicillium janczewskii*. Bioresour Technol **101**:4139-4143.

32. **Iembo T, da Silva R, Pagnocca FC, Gomes E**. 2002. Production, characterization, and properties of beta-glucosidase and beta-xylosidase from a strain of *Aureobasidium sp*. Appl Biochem Microbiol **38**:549-552.

33. **Knob A, Carmona EC**. 2009. Cell-associated acid beta-xylosidase production by *Penicillium sclerotiorum*. N Biotechnol **26**:60-67.

762 34. **Rasmussen LE, Sorensen HR, Vind J, Vikso-Nielsen A**. 2006. Mode of action
763 and properties of the beta-xylosidases from *Talaromyces emersonii* and
764 *Trichoderma reesei*. Biotechnol Bioeng **94**:869-876.

765 35. **Deshpande N, Wilkins MR, Packer N, Nevalainen H**. 2008. Protein
766 glycosylation pathways in filamentous fungi. Glycobiology **18**:626-637.

767 36. **Hayes BK, Varki A**. 1993. Biosynthesis of oligosaccharides in intact golgi
768 preparations from rat liver. Analysis of N-linked glycans labeled by UDP-[6-H-
769 3]Galactose, CMP-[9-H-3]N-acetylneuraminic acid, and [Acetyl-H-3]acetyl-
770 coenzyme A. Journal of Biological Chemistry **268**:16155-16169.

771 37. **Poutanen K, Puls J**. 1988. Characteristics of *Trichoderma reesei* beta-xylosidase
772 and its use in the hydrolysis of solubilized xylans. Appl Microbiol Biotechnol
773 **28**:425-432.

774 38. **Andrade SD, Polizeli MDLT, Terenzi HF, Jorge JA**. 2004. Effect of carbon
775 source on the biochemical properties of beta-xylosidases produced by *Aspergillus*
776 *versicolor*. Process Biochem **39**:1931-1938.

777 39. **Saha BC**. 2003. Purification and properties of an extracellular beta-xylosidase
778 from a newly isolated *Fusarium proliferatum*. Bioresour Technol **90**:33-38.

779 40. **Bin Y, Hongzhang C**. 2010. Effect of the ash on enzymatic hydrolysis of steam-
780 exploded rice straw. Bioresour Technol **101**:9114-9119.

781 41. **Eisenthal R, Danson MJ, Hough DW**. 2007. Catalytic efficiency and k_{cat}/K_m: a
782 useful comparator? Trends in Biotechnology **25**:247-249.

42. **Xu WZ, Shima Y, Negoro S, Urabe I**. 1991. Sequence and properties of beta-xylosidase from *Bacillus pumilus* Ipo. Contradiction of the previous nucleotide sequence. European Journal of Biochemistry **202**:1197-1203.

43. **Jordan DB, Wagschal K**. 2010. Properties and applications of microbial beta-D-xylosidases featuring the catalytically efficient enzyme from *Selenomonas ruminantium*. Appl Microbiol Biotechnol **86**:1647-1658.

44. **Herrmann MC, Vrsanska M, Jurickova M, Hirsch J, Biely P, Kubicek CP**. 1997. The beta-D-xylosidase of *Trichoderma reesei* is a multifunctional beta-D-xylan xylohydrolase. Biochem J **321**:375-381.

45. **Sunna A, Antranikian G**. 1997. Xylanolytic enzymes from fungi and bacteria. Crit Rev Biotechnol **17**:39-67.

46. **Juturu V, Wu JC**. 2014. Microbial Exo-xylanases: A Mini Review. Appl Biochem Biotechnol **174**:81-92.

47. **Dilokpimol A, Nakai H, Gotfredsen CH, Appeldoorn M, Baumann MJ, Nakai N, Schols HA, Abou Hachem M, Svensson B**. 2011. Enzymatic synthesis of beta-xylosyl-oligosaccharides by transxylosylation using two beta-xylosidases of glycoside hydrolase family 3 from *Aspergillus nidulans* FGSC A4. Carbohydr Res **346**:421-429.

48. **Mala S, Dvorakova H, Hrabal R, Kralova B**. 1999. Towards regioselective synthesis of oligosaccharides by use of alpha-glucosidases with different substrate specificity. Carbohydr Res **322**:209-218.

49. **Mozolowski G, Connerton I**. 2009. Characterization of a highly efficient heterodimeric xylosidase from *Humicola insolens*. Enzym Microb Technol **45**:436-442.

50. **Kiss T, Kiss L**. 2000. Purification and characterization of an extracellular beta-D-xylosidase from *Aspergillus carbonarius*. World J Microbiol Biotechnol **16**:465-470.

51. **Wakiyama M, Yoshihara K, Hayashi S, Ohta K**. 2008. Purification and properties of an extracellular beta-xylosidase from *Aspergillus japonicus* and sequence analysis of the encoding gene. J Biosci Bioeng **106**:398-404.

52. **Kumar S, Ramon D**. 1996. Purification and regulation of the synthesis of a beta-xylosidase from *Aspergillus nidulans*. FEMS Microbiol Lett **135**:287-293.

53. **Michelin M, Peixoto-Nogueira SC, Silva TM, Jorge JA, Terenzi HF, Teixeira JA, Polizeli MdL**. 2012. A novel xylan degrading beta-D-xylosidase: purification and biochemical characterization. World J Microbiol Biotechnol **28**:3179-3186.

54. **Hayashi S, Ohno T, Ito M, Yokoi H**. 2001. Purification and properties of the cell-associated beta-xylosidase from *Aureobasidium*. J Ind Microbiol Biotechnol **26**:276-279.

55. **Zanoelo FF, Polizeli MDTD, Terenzi HF, Jorge JA**. 2004. Purification and biochemical properties of a thermostable xylose-tolerant beta-D-xylosidase from *Scytalidium thermophilum*. J Ind Microbiol Biotechnol **31**:170-176.

56. **Katapodis P, Nerinckx W, Claeyssens M, Christakopoulos P**. 2006. Purification and characterization of a thermostable intracellular beta-xylosidase

826 from the thermophilic fungus *Sporotrichum thermophile*. Process Biochem
827 **41**:2402-2409.

828 57. **Guerfali M, Gargouri A, Belghith H**. 2008. *Talaromyces thermophilus* beta-D-
829 xylosidase: Purification, characterization and xylobiose synthesis. Appl Biochem
830 Biotechnol **150**:267-279.

831 58. **Matsuo M, Yasui T**. 1984. Purification and some properties of beta-xylosidase
832 from *Trichoderma viride*. Agricultural and Biological Chemistry **48**:1845-1852.

833 59. **Jordan DB, Wagschal K, Grigorescu AA, Braker JD**. 2013. Highly active beta-
834 xylosidases of glycoside hydrolase family 43 operating on natural and artificial
835 substrates. Appl Microbiol Biotechnol **97**:4415-4428.

836 60. **Wagschal K, Heng C, Lee CC, Robertson GH, Orts WJ, Wong DW**.
837 Purification and characterization of a Glycoside Hydrolase Family 43 beta-
838 xylosidase from *Geobacillus thermoleovorans* IT-08. Appl Biochem Biotechnol
839 **155**:304-313.

840 61. **Kirikyali N, Wood J, Connerton IF**. 2014. Characterisation of a recombinant
841 beta-xylosidase (xylA) from *Aspergillus oryzae* expressed in *Pichia pastoris*.
842 AMB Express **4**:68.

843 62. **Kirikyali N, Connerton I**. 2014. Heterologous expression and kinetic
844 characterisation of *Neurospora crassa* beta-xylosidase in *Pichia pastoris*. Enzym
845 Microb Technol **57**:63-68.

63. **Jordan DB**. 2008. B-D-xylosidase from *Selenomonas ruminantium*: Catalyzed reactions with natural and artificial substrates. Appl Biochem Biotechnol **146**:137-149.

FIGURES

FIGURE 1. Extracellular β-xylosidase activity (A) and protein concentration (B) of *T. amestolkiae* cultures in Mandels medium in the presence of different carbon sources.

FIGURE 2. Estimation of BxTW1 molecular mass by SDS-PAGE (A) and MALDI-TOF-MS (B). 1) Molecular mass standards, 2) BxTW1 treated with EndoH and, 3) glycosylated BxTW1.

FIGURE 3. Effect of temperature and pH on BxTW1 activity. A) The line indicates the effect of temperature on enzyme activity and bars show its stability in a range of temperatures from 30 ºC to 70 ºC after 72 h. B) The line corresponds to the effect of pH on enzyme activity and bars show its stability in a range of pH from 2.2 to 9 after 72 h.

FIGURE 4. Effect of some chemical compounds on BxTW1 activity.

FIGURE 5. A) Proton NMR spectra of xylotriose consumption by BxTW1 along time. Signals using for quantification are pointed. B) Evolution of xylotriose and xylobiose concentration during the reaction time. Concentrations were determined by integrating the appropriated signals of each compound.

FIGURE 6. Transxylosylation ratios according to the initial substrate concentration. Reaction products and substrate were separated by HPLC. Ratios were obtained from comparing areas under the curves of remaining substrate and product of transxylosylation.

FIGURE 7. A) Transxylosylation ratios of BxTW1 in the presence of different acceptors. Acceptor specificity is presented as a heat map based on transxylosylation

ratios. The hierarchical clustering analysis was performed using the clustergram algorithm within Matlab environment (MathWorks, Natick, MA). B) Hierarchical clustering of acceptors' chemical similarity estimated by Tanimoto coefficient calculation using Chemmine program. Clustering was performed within Matlab environment (MathWorks, Natick, MA).

879

880 **TABLE 1.** Kinetic parameters of BxTW1 against different substrates.

881

Substrate	K_m **(mM)**	V_{max} **(U/mg)**	k_{cat} **(s^{-1})**	k_{cat}/K_m **($mM^{-1}\cdot s^{-1}$)**
*p*NPX	0.17±0.01	52.0±0.5	173	1000
*p*NP-α-L-arabinopyranoside	3.6±0.3	66.9±4.2	220	62
*p*NP-α-L-arabinofuranoside	5.8±0.4	43.0±1.7	143	25
Xylobiose	0.48±0.05	55.2±1.3	183	380
Xylotriose	0.22±0.01	19.8±0.3	66.1	290
Xylotetraose	0.20±0.01	15.4±0.1	51.2	260
Xylopentaose	0.20±0.01	11.8±0.2	39.2	200
Xylohexaose	0.22±0.01	9.5±0.1	32	140
Substrate	K_m **(mg/mL)**	V_{max} **(U/mg)**	k_{cat} **(s^{-1})**	k_{cat}/K_m **($mM^{-1}\cdot s^{-1}$)**
Xylan	7.0±0.2	68.7±0.6	229	-

882

883

884 **TABLE 2.** Kinetic parameters for different fungal β-xylosidases using *p*NPX as model

885 substrate.

886

Organism	Enzyme	K_m (mM)	V_{max} (U/mg)	k_{cat} (s^{-1})	k_{cat}/K_m ($mM^{-1}·s^{-1}$)	Reference
Talaromyces amestolkiae	BxTW1	0.17	52.0	173	1000	This work
Aspergillus awamori	X-100	0.25	-	17.5	70	(49)
Aspergillus carbonarius		0.20	3.64	-	-	(50)
Aspergillus japonicus		0.31	114	215[a]	690[a]	(51)
Aspergillus nidulans		1.1	25.6	76.8[a]	70[a]	(52)
Aspergillus ochraceus		0.66	39	-	-	(53)
Aureobasidium spp.	Bxyl	2	940	5500	2750	(54)
Fusarium proliferatum		0.77	75	-	-	(39)
Fusarium verticilloides		0.85	-	-	-	(26)
Humicola grisea	Bxyl	0.48	-	-	-	(49)
	Bxyl	1.37	13.0	$1.22·10^{-5}$	$1·10^{-5}$	
Humicola insolens		1.74	22.2		3900	(49)
Penicillium sclerotium		0.78	0.51	1.2[a]	1.6[a]	(28)
Scytalidium thermophilum	Bxyl	1.7	88	66[a]	38.8[a]	(55)
Sporotrichum thermophile	Intracell Bxyl	1.1	114	89.3[a]	81[a]	(56)
Talaromyces emersonii	BXTE	0.06	-	0.017	0.3[a]	(34)
	Xyl I	0.13	1.7	430	3300	(49)
	Xyl II	32.9	6.3	900	27	
	Xyl III	1.4	0.26	61	44	
Talaromyces thermophilus	Bxyl	2.37	0.049	0.037[a]	0.016[a]	(57)
Trichoderma reesei	BXTR	0.8	-	0.015	0.02	(49)
Trichoderma viride		5.8	-	21.3	3.7	(58)

887

888 [a] Not included in the original article but calculated with the data provided.

889

890 **TABLE 3.** Catalytic efficiency against XOS from X2 to X3 of fungal and bacterial β-

891 xylosidases.

892

Organism	**Enzyme**	k_{cat}/K_m **(mM^{-1}·s^{-1})**					**Reference**
		X2	X3	X4	X5	X6	
Talaromyces amestolkiae	BxTW1	382	287	258	198	143	This work
Aspergillus nidulans	BxlA	70	58	42	33	22	(47)
	BxlB	14	9	8	5	4	
Alkaliphilus metalliredigens	AmX	39.4	30.7	-	-	-	(59)
Bacillus pumilus	BpX	7.45	6.10	1.42	-	-	
Bacillus subtilis	BsX	56.6	35.2	1.42	-	-	
Geobacillus thermoleovorans	GbtXyl43A	$5.1\cdot10^{-3}$	$3.9\cdot10^{-3}$	-	-	-	(60)
Lactobacillus brevis	LbX	138	80.8	2.40	-	-	(59)
Aspergillus oryzae[1]	XylA	13.8	9.7	33.1	-	-	(61)
Neurospora crassa[1]		3.4	1.4	0.7	-	-	(62)
Selenomonas ruminantium	SXA	90.2	44.8	33.3	27.0	26.1	(63)

893

894 [1]Recombinant protein expressed *in P. pastoris*

895

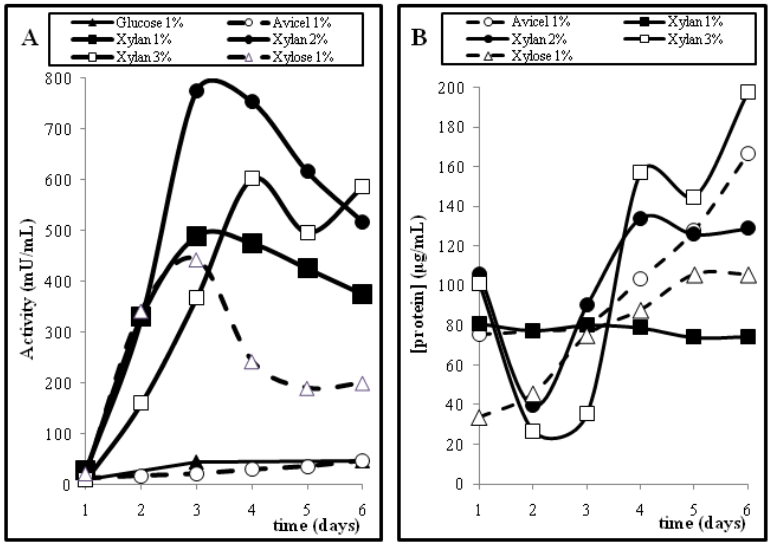

896

897 **FIG 1** Extracellular _-xylosidase activity (A) and protein concentration (B) of *T.*
898 *amestolkiae* cultures in Mandels medium in the presence of different carbonsources.
899

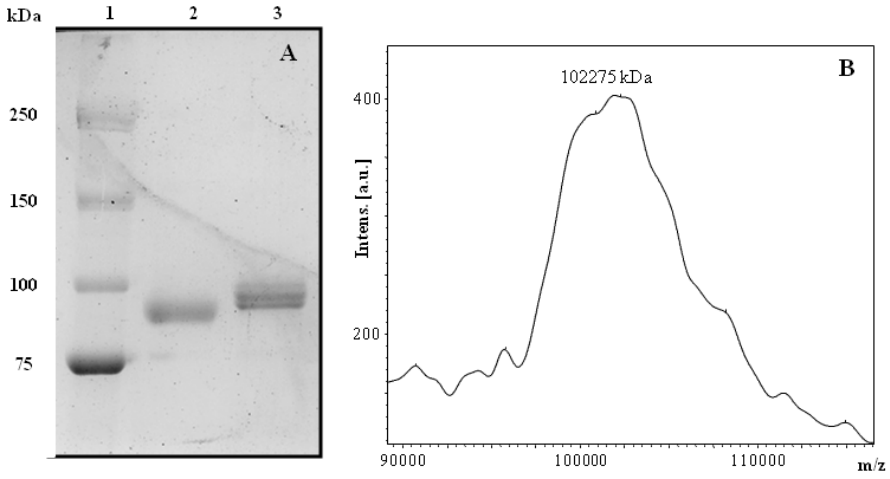

FIG 2 Estimation of BxTW1 molecular mass by SDS-PAGE (A) and MALDI-TOF MS (B). Lanes: 1, molecular mass standards; 2, BxTW1 treated with Endo H;3, glycosylated BxTW1. Intens., intensity; a.u., arbitrary units.

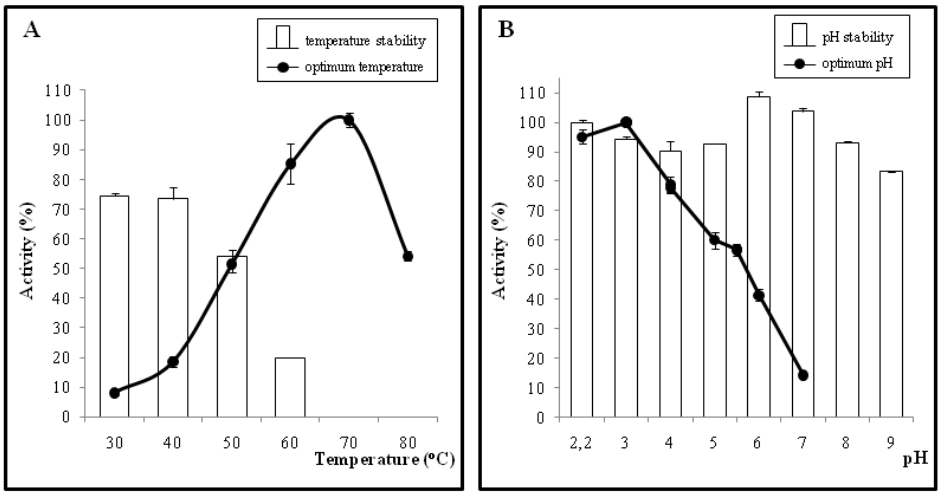

905
906 **FIG 3** Effect of temperature (A) and pH (B) on BxTW1 activity. (A) The line
907 indicates the effect of temperature on enzyme activity, and the bars show its stability
908 in a range of temperatures from 30°C to 70°C after 72 h. (B) The line corresponds to
909 the effect of pH on enzyme activity, and the bars show its stability in a range of pH
910 from 2.2 to 9 after 72 h.
911

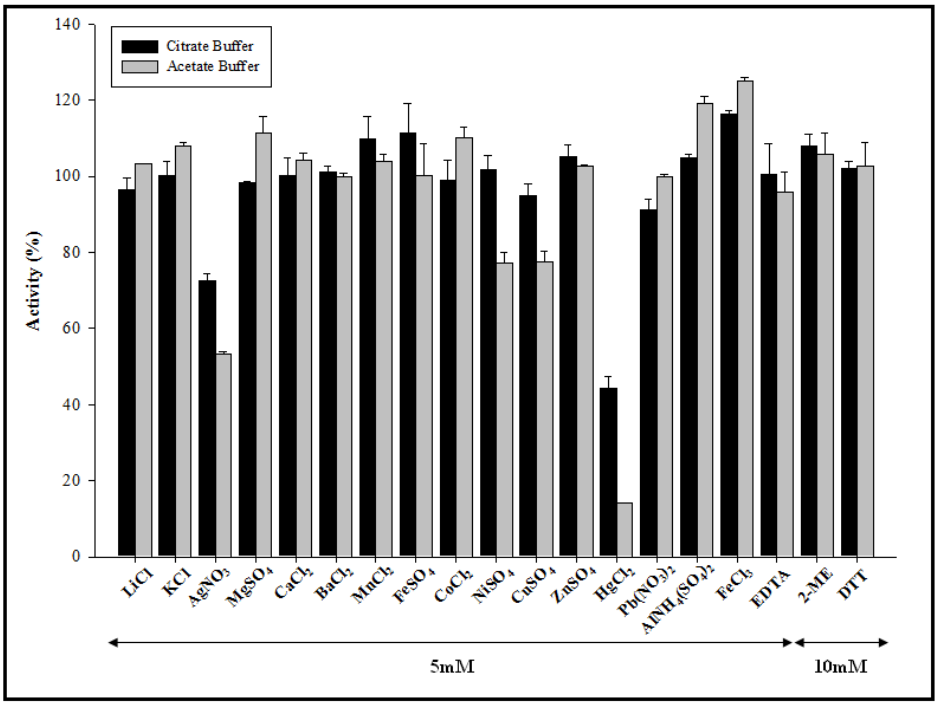

912
913 **FIG 4** Effects of some chemical compounds on BxTW1 activity.

914

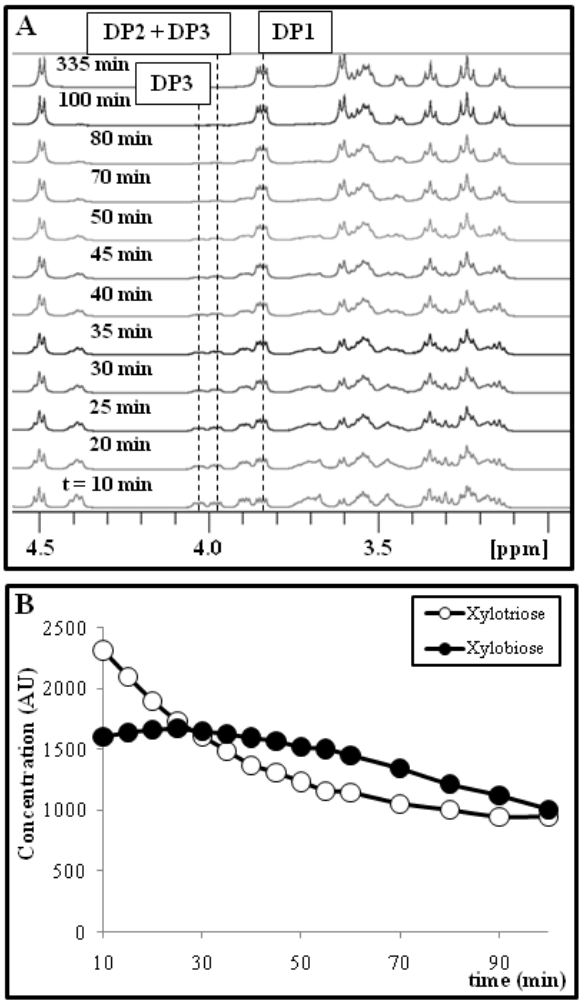

915

916 **FIG 5** (A) Proton NMR spectra of xylotriose consumption by BxTW1 over time.
917 Signals using for quantification are indicated by vertical dashed lines. (B) Evolution of
918 xylotriose and xylobiose concentration during the reaction time. Concentrations were
919 determined by integrating the appropriate signals of each compound.

920

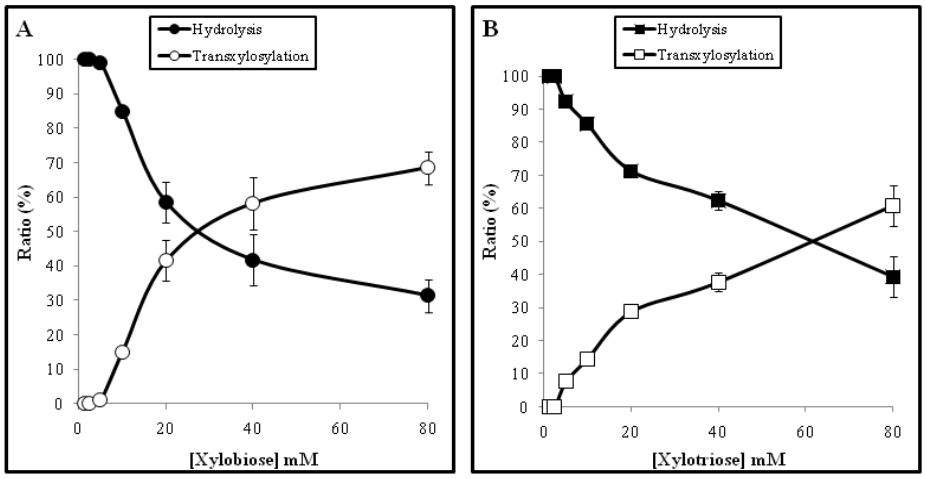

FIG 6 Transxylosylation ratios according to the initial substrate concentration. Reaction products and substrate were separated by HPLC. Ratios were obtained by comparing areas under the curves of the remaining substrate and the product of transxylosylation.

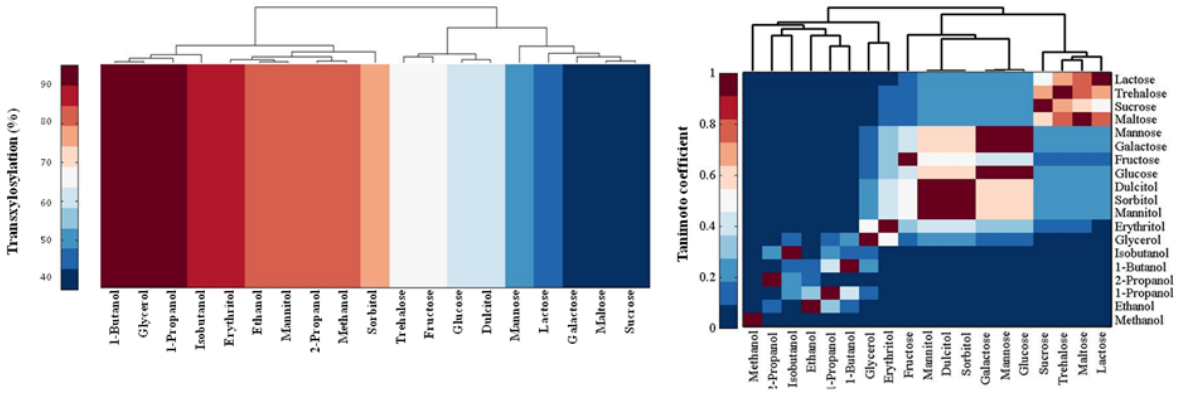

926
927 **FIG 7** (A) Transxylosylation ratios of BxTW1 in the presence of different acceptors.
928 Acceptor specificity is presented as a heat map based on transxylosylation ratios. The
929 hierarchical clustering analysis was performed using the clustergram algorithm within
930 the Matlab environment (MathWorks, Natick, MA). (B) Hierarchical clustering of the
931 chemical similarity of the acceptors as estimated by Tanimoto coefficient calculation
932 using the ChemMine program. Clustering was performed within the Matlab
933 environment.
934